ELSEVIER

International Journal of Solids and Structures 41 (2004) 3977–3997

INTERNATIONAL JOURNAL OF SOLIDS and STRUCTURES

www.elsevier.com/locate/ijsolstr

A p-type solution for the bending of rectangular, circular, elliptic and skew plates

T. Muhammad, A.V. Singh *

Department of Mechanical and Materials Engineering, The University of Western Ontario, Eng. Building Room 2059 A, London, Ont., Canada N6A 5B9

Received 20 February 2004; received in revised form 20 February 2004
Available online 25 March 2004

Abstract

An energy method is presented in this paper for the linear static analysis of first order shear deformable plates of various shapes. In this method, the displacement fields are defined in terms of the shape functions, which correspond to a set of predefined points and are composed of significantly high order polynomials. The positions of these points are calculated by mapping the geometry using naturalized coordinates and the interpolating shape functions of second order to fourth order polynomials. The displacement degrees of freedom are assigned to each of the displacement nodes. The method is evaluated using the fully clamped and simply supported rectangular, circular and elliptic plates subjected to uniformly distributed transverse load as examples for which the exact results are given in the monograph of Timoshenko and Woinowsky-Krieger. Also presented in this paper is the analysis of the above three types of plates subjected to eccentric square and circular patch loadings. Plates with eccentric square and circular openings are analyzed by this method using the full plate model and the results compare extremely well with those obtained by finite element methods. The cutout part of the plate is accommodated in the solution by superposing negative stiffness and load over the area of the opening. Finally, skew plates with simply supported and clamped boundaries are analyzed and discussed.

Keywords: p-type formulation; Plate with cutout; Circular; Elliptic; Rectangular and skew plates

1. Introduction

The plate bending problems have been studied by great mathematicians and engineers of the last two centuries. During the second half of the last century, the finite element method became the widely accepted solution method for engineering problems and is being developed further for new applications and improved accuracy. In the common version of the finite element method, the problem is solved using low

* Corresponding author. Tel.: +1-519-661-2111; fax: +1-519-661-3020.
E-mail address: avsingh@eng.uwo.ca (A.V. Singh).

0020-7683/$ - see front matter © 2004 Elsevier Ltd. All rights reserved.
doi:10.1016/j.ijsolstr.2004.02.047

order elements and the accuracy in the result is obtained through mesh refinement. This is the *h*-version of the finite element method. Then the *h–p* version, also referred to as the hierarchical finite method, was introduced during the seventies and early eighties of the last century. In this method mesh of a fixed order finite element is used for the solution and the convergence is sought by increasing the degrees of the elements, while a constant mesh is maintained during the analysis. Bardell (1996) published a paper intending to extend the application of the *h–p* method for the analysis of an Euler–Bernoulli beam and to emphasize the engineering approach rather than the mathematical procedure.

Recently, researchers have shown significant amount of interest in the numerical solution of engineering problems without using a mesh. Belytschko et al. (1994, 1996) have published a series of papers on element free Galerkin method. A method using a meshless spatial approximation based only on nodes was used by El Ouatouati and Johnson (1999) to derive the stiffness and mass matrices for a three-dimensional simply connected elastic body. Suetake (2002) proposed a simple element free method using Lagrange polynomial without employing the moving least squares (MLS) and discussed solutions of elastic beam and plate problems. A least squares approach was used by Mohr (2000) for the approximate polynomial solutions for simply supported equilateral triangular and square plates. Chen et al. (2003) proposed an element free Galerkin method for the free vibration analysis of laminated composite plates. They studied square, elliptical and perforated plate as numerical examples.

The present work also deals with the meshless solution of plate bending problems using a single algorithm based on the variational principles modified such that various shaped plates can be analyzed. The method has been used to solve rectangular, circular, elliptical, and skew plate bending problems with simply supported and clamped boundary conditions. Load cases considered herein include: uniform load on the entire plate, or circular and rectangular eccentric patch loads. Both full plate and the one with an eccentric opening are analyzed successfully. There is some limited number of published work using different methods for this type of plate bending problems. Ollerton (1976) reported bending stresses in thin circular plates having a single eccentric hole and mixtures of clamped and simply supported boundaries. The load cases considered were: a concentrated force uniformly distributed round the inner boundary, moments about two perpendiculars axes, and uniform pressure on the plate surface. An exact method of solution was presented by Harik and Salamoun (1986) for rectangular plates subjected to uniform, patch, line and point loads and with clamped and simply supported along two parallel edges and any combination of boundary conditions along the remaining edges. Plates subjected to line and patch loads were also studied by Venkatesh and Jirousek (1995) using hybrid-Trefftz element, the assumed displacement field of which satisfied the differential equilibrium conditions while the conformity was imposed in a weighted residual sense. Liew and Han (1997) used differential quadrature method (DQM) to the bending analysis of simply supported shear deformable skew plates subjected to uniformly distributed surface load.

In the present study, the plate geometry is defined using a number of grid points of prescribed coordinates and then the natural coordinates are used to derive the shape functions, which can be used in interpolating the Cartesian coordinates of a point on and within the plate boundary. The displacement field is introduced in Cartesian coordinates using very high order polynomials in comparison with those that are used for the geometry. Depending upon the order of the displacement field functions, a set of nodal points is generated using the geometric shape functions. Then the displacement shape functions in terms of Cartesian coordinates are derived associated with each displacement node and used further for obtaining the stiffness matrix and the load vectors. Numerical integration is performed in Cartesian system using a large number of Gauss points and corresponding weights. To accommodate the opening in the plate, the negative stiffness and loads over the area of the opening are superposed to the full plate equations. Numerical results from the present method are compared with the exact (Timoshenko and Woinowsky-Krieger, 1959) and finite element (I-DEAS) solutions. Additionally, clamped and simply supported skew plates are investigated and results are compared with those published by Morley (1963). The method is simple, efficient and capable of yielding very accurate results for both displacement and stress.

2. Elastic plate equations

The equations in this section are based on the Reissner–Mindlin theory of plates that is also known as the first order shear deformation theory. The displacement components along the Cartesian axes at an arbitrary point in the plate are denoted by u', v', and w' respectively and are expressed as:

$$u' = u + z\beta_1, \quad v' = v + z\beta_2, \quad w' = w. \tag{1}$$

In the above equations, symbols u, v, and w denote the displacement components at the middle plane of the plate in x, y, and z directions respectively; β_1 and β_2 are the components of rotation of the normal to the middle plane that is also referred to as the reference plane; and z is the distance measured from the reference plane in the direction perpendicular to the plate. For the plate bending problems, the in-plane displacement components u and v are assumed to be zero i.e. no stretching of the middle plane. After dropping u and v from Eq. (1), it can be expressed in the matrix form as

$$\{u'\} = [Z_1]\{\Delta\}, \tag{2}$$

where

$$\{u'\}^{\mathrm{T}} = \{\, u' \quad v' \quad w' \,\}, \quad \{\Delta\}^{\mathrm{T}} = \{\, w \quad \beta_1 \quad \beta_2 \,\},$$

and

$$[Z_1] = \begin{bmatrix} 0 & z & 0 \\ 0 & 0 & z \\ 1 & 0 & 0 \end{bmatrix}.$$

The strain–displacement relationship is derived as:

$$\{\varepsilon'\} = [Z]\{X\}, \tag{3}$$

where

$$\begin{aligned} &\{\varepsilon'\}^{\mathrm{T}} = \left\{ \varepsilon'_x \quad \varepsilon'_y \quad \gamma'_{xy} \quad \gamma'_{yz} \quad \gamma'_{zx} \right\}, \\ &\{X\}^{\mathrm{T}} = \{\, \gamma_{yz} \quad \gamma_{zx} \quad \kappa_x \quad \kappa_y \quad \kappa_{xy} \,\}, \\ &\gamma_{yz} = \frac{\partial w}{\partial y} + \beta_2, \quad \gamma_{zx} = \frac{\partial w}{\partial x} + \beta_1, \\ &ak_x = \frac{\partial \beta_1}{\partial x}, \quad ak_y = \frac{\partial \beta_2}{\partial y}, \quad ak_{xy} = \frac{\partial \beta_1}{\partial y} + \frac{\partial \beta_2}{\partial x}, \end{aligned} \tag{4}$$

$$[Z] = \begin{bmatrix} 0 & 0 & z & 0 & 0 \\ 0 & 0 & 0 & z & 0 \\ 0 & 0 & 0 & 0 & z \\ 1 & 0 & 0 & 0 & 0 \\ 0 & 1 & 0 & 0 & 0 \end{bmatrix}, \quad [d]^{\mathrm{T}} = \begin{bmatrix} \dfrac{\partial}{\partial y} & \dfrac{\partial}{\partial x} & 0 & 0 & 0 \\ 0 & 1 & \dfrac{\partial}{\partial x} & 0 & \dfrac{\partial}{\partial y} \\ 1 & 0 & 0 & \dfrac{\partial}{\partial y} & \dfrac{\partial}{\partial x} \end{bmatrix}.$$

In the above equation, displacement (w) and coordinates (x, y) are normalized with respect to one of the plate's principal dimensions, e.g. the length (a) of a rectangular plate or the major axis (a) of an elliptic plate. This provides non-dimensional form to the above equations.

The strain–curvature vector, $\{X\}$ is further expressed as

$$\{X\} = [d]\{\Delta\}. \tag{5}$$

Strain energy under a given state of stress (or strain) for an infinitesimal volume $\mathrm{d}x\,\mathrm{d}y\,\mathrm{d}z$ is given by

$$\mathrm{d}U = \frac{1}{2}\{\varepsilon'\}^{\mathrm{T}}[E]\{\varepsilon'\}\,\mathrm{d}x\,\mathrm{d}y\,\mathrm{d}z \quad \text{or} \quad \mathrm{d}U = \frac{1}{2}\{X\}^{\mathrm{T}}[Z]^{\mathrm{T}}[E][Z]\{X\}\,\mathrm{d}x\,\mathrm{d}y\,\mathrm{d}z. \tag{6}$$

In the above, matrix $[E]$ is the fifth order and composed of the elastic modulus (E) and the Poisson's ratio (v). Its non-zero terms are as follows.

$$E_{11} = E_{22} = \frac{E}{1-v^2}, \quad E_{12} = E_{21} = vE_{11}, \quad E_{33} = \frac{E}{2(1+v)}, \quad \text{and} \quad E_{44} = E_{55} = kE_{33}. \tag{7}$$

The shear correction factor ($k = 5/6$) is used in the matrix to compensate for the parabolic distribution of the transverse shear stress along the thickness of the plate. Integration of Eq. (6) over the thickness of the plate, gives

$$U = \frac{1}{2}\iint_{\text{Area}} \{X\}^{\mathrm{T}}[D]\{X\}\,\mathrm{d}x\,\mathrm{d}y, \tag{8}$$

where $[D]_{8\times 8}$ is composed of the thickness and elastic properties of the plate.

$$[D] = \int_{-\frac{h}{2}}^{+\frac{h}{2}} [Z]^{\mathrm{T}}[E][Z]\,\mathrm{d}z. \tag{9}$$

The non-zero terms in $[D]_{5\times 5}$ are given below.

$$\begin{aligned} &D_{11} = D_{22} = (1/2)(1-v)kK_0, \quad D_{33} = D_{44} = D_0, \\ &D_{34} = D_{43} = vD_0, \quad D_{55} = \left(\frac{1-v}{2}\right)D_0, \\ &K_0 = \frac{Eh}{1-v^2}, \quad D_0 = \frac{Eh^3}{12(1-v^2)}. \end{aligned} \tag{10}$$

A numerical solution procedure is developed in this investigation for the analysis of plate bending problems. The method is described below in various steps.

Displacement fields. A quadrilateral region with four curved edges defines the geometry of the plate in x–y plane as shown in Fig. 1. The region represents the middle surface of the plate with the thickness (h) which is assumed to be uniform and small in comparison with the other dimensions along x and y axes.

Fig. 1 shows 9 points which represent the geometric nodes at the middle plane and their coordinates (x_i, y_i) with $i = 1, 2, 3, \ldots, 9$ are prescribed. The shape functions $N_i(\xi, \eta)$ with $i = 1, 2, 3, \ldots, 9$ are used for the interpolation of coordinates (x, y) of an arbitrary point inside the quadrilateral region, (Weaver and Johnston, 1984). The dimensionless coordinates ξ and η that are also known as natural coordinates are bounded by $-1 \leqslant (\xi, \eta) \leqslant +1$. The coordinates (x, y) can be interpolated by the following equations.

$$\begin{aligned} x(\xi,\eta) &= \sum_{i=1}^{9} N_i(\xi,\eta)x_i, \\ y(\xi,\eta) &= \sum_{i=1}^{9} N_i(\xi,\eta)y_i. \end{aligned} \tag{11}$$

The above interpolating scheme will be used in setting up the displacement fields in the following manner.

The displacement field is defined by high order polynomials in comparison with the ones used for the geometric interpolation. Only one displacement field defines the displacement components (w, β_1, β_2) in whole region of the plate. In other words the high order polynomials represent the displacement field of the whole plate as one element. A different set of nodes is introduced and each node has three degrees of

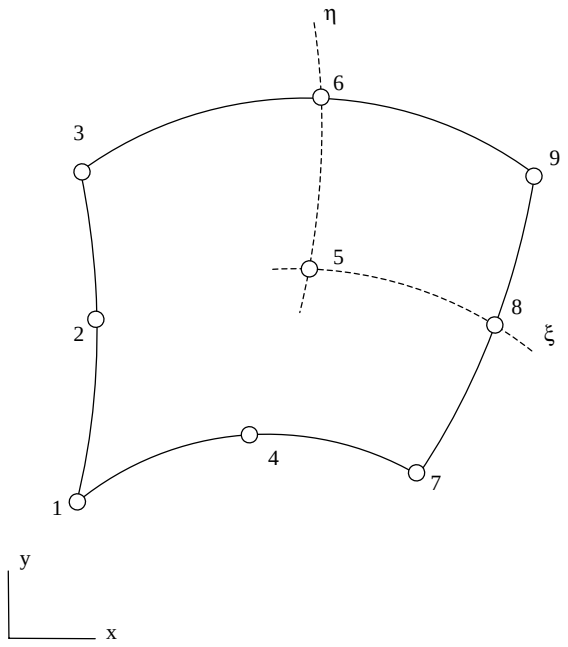

Fig. 1. A quadrilateral boundary represented by nine points.

freedom corresponding to w, β_1, and β_2. The x and y coordinates of the displacement nodes are obtained using the geometric interpolation equation (11). The values of these three components are interpolated by the following equations.

$$\begin{aligned} w &= \sum_{i=1}^{n} f_i(x,y) W_i, \\ \beta_1 &= \sum_{i=1}^{n} f_i(x,y) \theta_i, \\ \beta_2 &= \sum_{i=1}^{n} f_i(x,y) \phi_i. \end{aligned} \tag{12}$$

In the above equations, $f_i(x,y)$ is the displacement shape function and the indices W_i, θ_i, and ϕ_i represent w, β_1, and β_2 respectively at the ith displacement node. The displacement nodes are introduced in the whole plate region using Eq. (11) which involves polynomials in each ξ and η. If p and q denote the orders of the polynomials in x and y, the number of displacement nodes required is: $n = (p+1)(q+1)$. Eq. (12) can be expressed in matrix form as

$$\{\Delta\}^{\mathrm{T}} = [\,[f_1(x,y)] \quad [f_2(x,y)] \quad [f_3(x,y)] \quad \cdots \quad \cdots \quad [f_n(x,y)]\,], \{\Gamma\} \tag{13}$$

where $\{\Delta\}^{\mathrm{T}} = \{\, w \quad \beta_1 \quad \beta_2 \,\}$,

$$\{\Gamma\}^{\mathrm{T}} = \{\, W_1 \quad \theta_1 \quad \phi_1 \quad W_2 \quad \theta_2 \quad \phi_2 \quad \cdots \quad W_n \quad \theta_n \quad \phi_n \,\}.$$

Matrix $[f_i(x,y)]_{3\times 3}$ is given below.

$$[f_i(x,y)] = \begin{bmatrix} f_i(x,y) & 0 & 0 \\ 0 & f_i(x,y) & 0 \\ 0 & 0 & f_i(x,y) \end{bmatrix}. \tag{14}$$

Substituting Eq. (14) into Eq. (5), we can write

$$\{X\} = [d][f_i(x,y)]\{\Gamma\} = [B]\{\Gamma\}, \tag{15}$$

where $[B]_{3\times n} = [d][f_i(x,y)]$ and is not presented in its detailed form because of large size.

Using Eq. (15), the strain energy expression can be written as

$$U = \tfrac{1}{2}\{\Gamma\}^{\mathrm{T}}[K]\{\Gamma\}. \tag{16}$$

In the above equation, matrix $[K]$ represents the stiffness matrix of the whole plate and can be expressed as

$$[K] = \int_{x_1}^{x_2}\int_{y_1(x)}^{y_2(x)} [B]^{\mathrm{T}}[D][B]\,\mathrm{d}y\,\mathrm{d}x. \tag{17}$$

Integration of the above expression for the stiffness matrix covering the entire domain of the plate will be carried out numerically using the Gauss-method. In this integration method the number of integration points and corresponding weights depends on the order of polynomial used to define the displacement field. The plate subjected to distributed loads will be solved with the help of load vectors that can be derived in the following manner.

Consistent load vector. Consider the plate subjected to a uniformly distributed transverse load of intensity p_0 on the plate as shown in Fig. 1. The work-done by this load against the plate under the assumed displacement field can be expressed as

$$W = \int\int_{\mathrm{Area}} p_0 w\,\mathrm{d}x\,\mathrm{d}y = p_0 \sum_{i=1}^{n} W_i \int_{x_1}^{x_2}\int_{y_1(x)}^{y_2(x)} f_i(x,y)\,\mathrm{d}y\,\mathrm{d}x. \tag{18}$$

Functions $y_1(x)$ and $y_2(x)$ represent the lower and upper boundaries respectively of the plate. In the above expression, the load vector $\{p\}$ that is composed of the load components associated with each W_i can be expressed as

$$\{p\} = p_0 \int_{x_1}^{x_2}\int_{y_1(x)}^{y_2(x)} f_i(x,y)\,\mathrm{d}y\,\mathrm{d}x. \tag{19}$$

Integration will be done using the same Gaussian quadrature method. Eq. (18) can be written in the vector form as

$$W = \{W_i\}^{\mathrm{T}}\{p\} \tag{20}$$

The variation of the above is given below.

$$\delta W = \{\delta\Gamma\}^{\mathrm{T}}\{p\}. \tag{21}$$

The above equation will be used in the equilibrium equation.

Equilibrium condition. The work-energy principle is used to derive the equilibrium equation. If potential energy of the plate is denoted by Π, then we can write $\Pi = U - W$. Where, U and W respectively are the strain energy of the plate and the work-done on the plate under the assumed displacement field. For the stable equilibrium of the plate the potential energy must be at a minimum. That means $\delta\Pi = 0$, which is expressed below.

$$\{\delta\Gamma\}^{\mathrm{T}}([K]\{\Gamma\} - \{p\}) = 0. \tag{22}$$

The solution of the above equation gives the displacement components of the plate at each displacement node.

Analysis of the plate with an opening. Here, like the above case of plates (i.e. without hole), the whole plate region is considered as one element. First the plate is considered to be without hole and the stiffness matrix of the whole region of the plate is calculated by using Eq. (17). The stiffness matrix of the plate without hole is expressed as

$$[K_1] = \int_{x_1}^{x_2}\int_{y_1(x)}^{y_2(x)} [B]^{\mathrm{T}}[D][B]\,\mathrm{d}x\,\mathrm{d}y. \tag{23}$$

The geometry in Fig. 2 is the same as of Fig. 1 except it has an opening with an arbitrary shape. All the equations derived in the above section of the paper will be used for the analysis of the plate with holes. The stiffness matrix of the opening is found by using Eq. (17), but with different integration limits. As shown in Fig. 2, the integration limit in the x direction is from x_3 to x_4 while the integration limit in the y direction is defined by the equation of the curve that defines the shape of the opening. So the stiffness matrix of the opening can be expressed by the following equation.

$$[K_2] = \int_{x_3}^{x_4}\int_{g_1(x)}^{g_2(x)} [B]^{\mathrm{T}}[D][B]\,\mathrm{d}y\,\mathrm{d}x. \tag{24}$$

It should be noted that integration in Eq. (24) is carried over the area of the patch or the hole. Matrices $[K_1]$ and $[K_2]$ are of the same order, as the same functions are used in both cases.

Now a new stiffness matrix is introduced that is equivalent to the stiffness matrix of the plate with hole. This matrix is nothing, but the difference of matrices $[K_1]$ and $[K_2]$. In this paper it is referred to as the "*equivalent stiffness matrix*".

$$[K_e] = [K_1] - [K_2]. \tag{25}$$

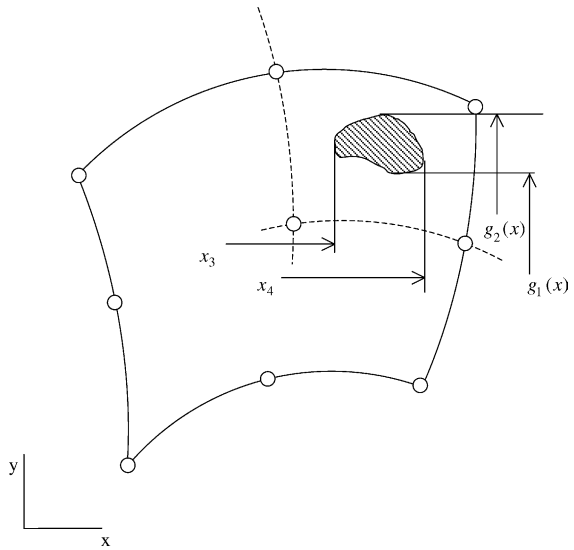

Fig. 2. Patch (or hole) shown in a quadratic domain.

Uniformly distributed load acting in the transverse direction of the plate can be expressed as

$$\{p_1\} = p_0 \int_{x_1}^{x_2} \int_{y_1(x)}^{y_2(x)} f_i(x,y)\,\mathrm{d}y\,\mathrm{d}x, \tag{26}$$

$$\{p_2\} = p_0 \int_{x_3}^{x_4} \int_{g_1(x)}^{g_2(x)} f_i(x,y)\,\mathrm{d}y\,\mathrm{d}x. \tag{27}$$

In the above expressions, vectors $\{p_1\}$ and $\{p_2\}$ correspond to the load acting on the whole plate without opening and only on the region of the hole, respectively. Now a new load vector is introduced, which acts on the plate with opening. This vector is, in fact, the difference of vectors $\{p_1\}$ and $\{p_2\}$. Again, it is called as the "*equivalent load vector*" and expressed as follows.

$$[p_e] = [p_1] - [p_2]. \tag{28}$$

For the equilibrium condition, Eq. (22) is used with new stiffness and load vectors. That can be written as

$$\{\delta\Gamma\}^{\mathrm{T}}([K_e]\{\Gamma\} - \{p_e\}) = 0. \tag{29}$$

The solution of the above equation gives the displacement components over the whole plate region, including the hollow part of the plate. The displacement components within the opening region are fictitious. The displacement and stress components are obtained by using interpolation functions.

3. Numerical results

The method presented in this paper is applied to the linear static analysis of rectangular, circular, elliptical and skew plates subjected to the uniformly distributed load over the entire plate or over a patch of the plate geometry. In case of the plate with an opening, the plate is assumed to be loaded uniformly over its surface area and the hole is incorporated in the analysis through negative stiffness and load parameters, as discussed earlier in this paper. A computer program has been developed in object oriented C++ computing environment with double precision. Shown in Figs. 3 and 4 are rectangular and elliptical plates respectively with circular and rectangular patches (or holes). A typical patch (or hole) is defined by its geometric center located at(x_0, y_0) as shown. The circular patch/hole is further defined by its radius R. Similarly, the rectangular patch/hole is defined by its sides c and d. The geometry of the rectangular and skew plates is defined using 9 points and the same number of shape functions, Eq. (11). Similarly, the geometries of circular and elliptical plates are defined by 9, 16 and 25 points for which quadratic, cubic and fourth order polynomials respectively in each of ξ and η directions are used. Eq. (11) is then used to find the Cartesian coordinates of the displacement grid points, which are further used in Eq. (12) for the displacement shape functions. For generating the shape functions given in Eq. (12) equal values for both p and q are used in the following calculations. It is found that the use of the fourth order polynomials yields very accurate representation of the circular region which is represented by 25 geometric nodes as shown in Fig. 5. Numerical results obtained from the present method are compared with the exact results (Timoshenko and Woinowsky-Krieger, 1959). Results for the cases with patch loadings and holes are obtained by the present method and then compared with those obtained by a commercial computer code I-DEAS. The value of the Poisson's ratio $v = 0.3$ is used in the following calculations.

Rectangular plate. The method is evaluated on uniformly loaded rectangular plates of length a and width b with clamped and simply-supported edges for which the numerical results are available in the monograph of Timoshenko and Woinowsky-Krieger (1959). Values of the geometric and material's parameters used in the calculation are: $a = 1.0$ (m), $E = 1.0$ (MPa), $h = 0.01$ (m) and $q = 1.0$ (Pa). Tenth order polynomial in

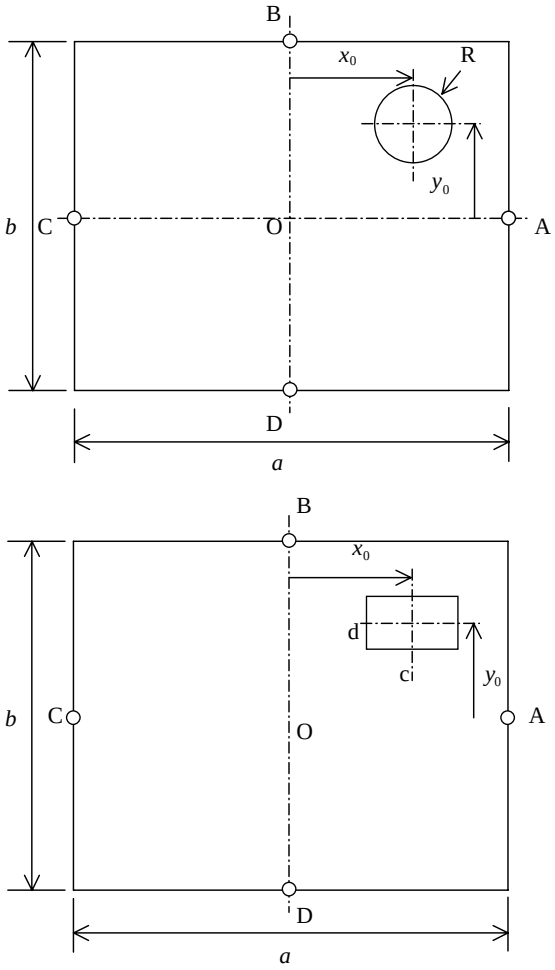

Fig. 3. Rectangular plate showing circular and rectangular patches (or holes).

each of x and y is used in defining the displacement fields corresponding to (w, β_1, β_2). This order of polynomials requires 121 displacement nodes and 363th order matrix to obtain displacement. Displacement restraints are applied to the nodes that lie on the boundary. Table 1 contains results pertaining to the transverse deflection at the center of the plate and bending moments at the center as well as the middle points A and B as shown in Fig. 3, of the edges for the uniformly loaded rectangular plates with built in edges from the two sources mentioned above. The aspect ratio (b/a) in this table varies from 1.0 to 2.0. A similar set of results is presented in Table 2 for the simply-supported case with aspect ration (b/a) varying from 1.0 to ∞. It is seen that the present method yields results, which are in excellent agreement with the exact results (Timoshenko and Woinowsky-Krieger, 1959).

Square plate with square or circular opening. For this case, the length of the plate $a = 1$ (m), thickness $h = 0.01$ (m), $E = 1$ (MPa), $v = 0.3$, the load magnitude of $q = 1.0$ (Pa), radius $r = 0.075$ (m) for the circular opening and center at (0.25 m, 0.25 m) are chosen for the calculation. It is expected that a doubly connected plate of this type will require very high order polynomials for the displacement fields to obtain accurate results. Also, for this type of plate numerical results are not readily available in the open literature.

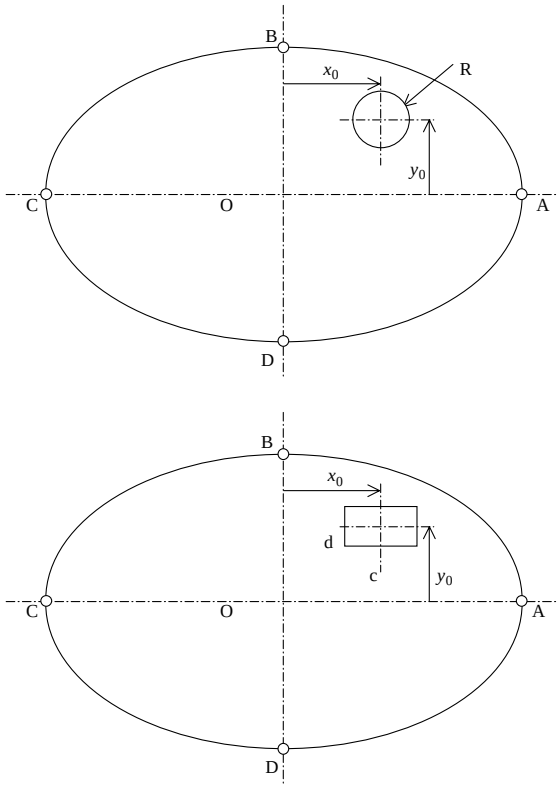

Fig. 4. Elliptic plate, with major and minor axes being 2a and 2b respectively, showing circular and rectangular patches (or holes).

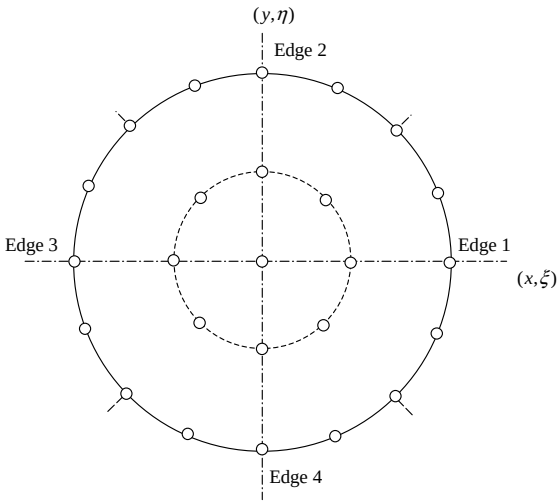

Fig. 5. Geometric grid for the circular region represented by a fourth order interpolating polynomials.

Table 1
Deflections (m) and bending moments (N m/m) in a uniformly loaded rectangular plate with built in edges

b/a	Displacement w_0		$(M_x)_A$		$(M_y)_B$	
	Present	Exact	Present	Exact	Present	Exact
1.0	0.0138	0.0138	−0.0514	−0.0513	−0.0514	−0.0513
1.1	0.0165	0.0164	−0.0582	−0.0581	−0.0539	−0.0538
1.2	0.0189	0.0188	−0.0640	−0.0639	−0.0554	−0.0554
1.3	0.0209	0.0209	−0.0688	−0.0687	−0.0563	−0.0563
1.4	0.0226	0.0226	−0.0727	−0.0726	−0.0568	−0.0568
1.5	0.0240	0.0240	−0.0758	−0.0757	−0.0570	−0.0571
1.6	0.0252	0.0251	−0.0782	−0.0780	−0.0571	−0.0571
1.7	0.0252	0.0260	−0.0800	−0.0799	−0.0571	−0.0571
1.8	0.0268	0.0267	−0.0813	−0.0812	−0.0571	−0.0571
1.9	0.0273	0.0272	−0.0823	−0.0822	−0.0570	−0.0571
2.0	0.0277	0.0277	−0.0830	−0.0829	−0.0570	−0.0571
			$(M_x)_0$		$(M_y)_0$	
			Present	Exact	Present	Exact
1.0			0.0229	0.0231	0.0229	0.0231
1.1			0.0267	0.0264	0.0232	0.0231
1.2			0.0300	0.0299	0.0228	0.0228
1.3			0.0327	0.0327	0.0222	0.0222
1.4			0.0350	0.0349	0.0213	0.0212
1.5			0.0368	0.0368	0.0203	0.0203
1.6			0.0382	0.0381	0.0193	0.0193
1.7			0.0393	0.0392	0.0183	0.0182
1.8			0.0401	0.0401	0.0174	0.0174
1.9			0.0407	0.0407	0.0165	0.0165
2.0			0.0412	0.0412	0.0158	0.0158

Table 2
Deflections (m) and bending moments (N m/m) in a uniformly loaded rectangular plate with simply supported edges

b/a	Present $(w)_0$	Exact $(w)_0$	Present $(M_x)_0$	Exact $(M_x)_0$	Present $(M_y)_0$	Exact $(M_y)_0$
1.0	0.0444	0.0443	0.0479	0.0479	0.0479	0.0479
1.1	0.0532	0.0530	0.0555	0.0553	0.0493	0.0494
1.2	0.0617	0.0616	0.0627	0.0626	0.0501	0.0501
1.3	0.0698	0.0697	0.0694	0.0693	0.0503	0.0504
1.4	0.0774	0.0770	0.0755	0.0753	0.0502	0.0506
1.5	0.0844	0.0843	0.0812	0.0812	0.0498	0.0499
1.6	0.0908	0.0906	0.0862	0.0862	0.0493	0.0493
1.7	0.0965	0.0964	0.0908	0.0908	0.0486	0.0486
1.8	0.1018	0.1017	0.0948	0.0948	0.0479	0.0479
1.9	0.1065	0.1064	0.0985	0.0985	0.0471	0.0471
2.0	0.1106	0.1106	0.1017	0.1017	0.0464	0.0464
3.0	0.1336	0.1336	0.1189	0.1189	0.0406	0.0404
4.0	0.1400	0.1400	0.1235	0.1235	0.0384	0.0384
5.0	0.1416	0.1416	0.1245	0.1246	0.0375	0.0375
∞	0.1481	0.1422	0.1301	0.1250	0.0390	0.0375

Therefore, the present formulation is evaluated against the typical finite element analysis (FEA) using eight-node mapped element from I-DEAS. Before proceeding with further cases, a convergence study is carried out for a clamped uniformly loaded plate with a circular opening in its first quadrant. Table 3

Table 3
Convergence study for a uniformly loaded square plate with built in edges and a circular opening at $(x_0, y_0) = (0.25, 0.25)$

Present method			I-DEAS		
$n(p)$	w_0 (m)	$(\sigma_{xx})_0$ (Pa)	n (NEL)	w_0 (m)	$(\sigma_{xx})_0$ (Pa)
25(4)	−0.0144	−1643.07	453(112)	−0.01379	−1413.0
36(5)	−0.0144	−1639.31	670(175)	−0.01379	−1396.0
49(6)	−0.0137	−1373.64	929 (252)	−0.01379	−1387.0
64(7)	−0.0137	−1374.38	1230(343)	−0.01379	−1387.0
81(8)	−0.0137	−1376.94			
100(9)	−0.0137	−1376.99			
121(10)	−0.0137	−1376.87			
144(11)	−0.0137	−1376.97			
169(12)	−0.0137	−1372.52			
196(13)	−0.0137	−1372.74			
225(14)	−0.0138	−1369.52			
256(15)	−0.0137	−1362.52			

contains values of the deflection and bending stresses at the center of the plate against the number of the displacement nodes (n), with the order of the polynomial (p or q) in the parenthesis. The results are converging for the deflection w_0 as well as the stress $(\sigma_{xx})_0$. Stress $(\sigma_{yy})_0$ is found equal to $(\sigma_{xx})_0$ in the calculation and hence not presented here. Similar convergence study is shown for the case of the FEA in this table. The indicator used for the convergence is again the number of nodal points (n) used in the FE model and the number of elements (NEL) is given in the parenthesis.

Values of the stresses obtained from the present method and the FEA at various locations, i.e. the middle points A–D of the edges and the center O as shown in Fig. 3, are presented in Table 4 for the case of fully clamped square plate subjected to uniformly distributed load and having circular and square openings. It is seen that the normal stresses σ_{xx} and σ_{yy} are in excellent agreement. The shear stresses are found to be negligibly small compared to the normal stresses and hence are not included in the table. Fourteenth order polynomial in each of x and y is used in generating the displacement fields using 225 displacement nodes. Number of nodes used in the I-DEAS model is 2111. The deflection w_0 at the center of the fully clamped plate from the present study and the I-DEAS are -13.72×10^{-3} (m) and -13.83×10^{-3} (m) respectively for

Table 4
A uniformly loaded square plate with built in edges and a circular/square opening at $(x_0, y_0) = (0.25\text{ m}, 0.25\text{ m})$

Location (x, y)	I-DEAS σ_{xx}	Present σ_{xx}	I-DEAS σ_{yy}	Present σ_{yy}
Square hole				
0.50,0.0	2987.00	2981.24	900.80	894.37
−0.50,0.0	3056.00	3064.35	922.20	919.30
0.0,0.50	900.80	894.46	2987.00	2981.55
0.0,−0.50	922.20	919.26	3056.00	3064.18
0.0,0.0	−1383.00	−1368.53	−1383.00	−1368.49
Circular hole				
0.50,0.0	3000.00	2999.74	904.80	899.92
−0.50,0.0	3054.00	3067.20	921.80	920.16
0.0,0.50	904.80	900.03	3000.00	3000.10
0.0,−0.50	921.80	920.11	3054.00	3067.03
0.0,0.0	−1374.00	−1369.52	1374.00	−1369.52

$a = b = 1.0$ (m), $c = d = 0.15$ (m), $E = 1.0$ (MPa), $q = 1.0$ (Pa), $v = 0.3$ and $h = 0.01$ (m).

the square hole. Similarly, the results from the two sources for the circular hole are -13.76×10^{-3} (m) and -13.75×10^{-3} (m) respectively.

For the all sides simply supported case, the values of $w_0, (\sigma_{xx})_0$ and $(\sigma_{yy})_0$ are calculated at the center $(0.0, 0.0)$ and given in the following.

$$\begin{aligned}
\text{Square hole}: \quad & w_0 = -44.70\times10^{-3}\ (\text{m}), \quad (\sigma_{xx})_0 = (\sigma_{yy})_0 = -2862.74\ (\text{Pa}) \quad (\text{present}),\\
& w_0 = -44.93\times10^{-3}\ (\text{m}), \quad (\sigma_{xx})_0 = (\sigma_{yy})_0 = -2868.00\ (\text{Pa}) \quad (\text{I-DEAS}),\\
\text{Circular hole}: \quad & w_0 = -44.59\times10^{-3}\ (\text{m}), \quad (\sigma_{xx})_0 = (\sigma_{yy})_0 = -2863.11\ (\text{Pa}) \quad (\text{present}),\\
& w_0 = -44.93\times10^{-3}\ (\text{m}), \quad (\sigma_{xx})_0 = (\sigma_{yy})_0 = -2866.00\ (\text{Pa}) \quad (\text{I-DEAS}).
\end{aligned}$$

Stresses at the mid-edge points are found to be too small for this case to be presented.

Square plate with a square or circular patch loading. For this a square plate with uniform load p on a small square with $c = d = 0.25$ (m) and center located at (0.25 m, 0.25 m) is analyzed. Similarly, a square plate with uniform load p on a small circular area of radius $r = 0.125$ (m) and center at (0.25 m, 0.25 m) has been analyzed by both methods. Values of the stresses at middle points A–D of the edges of the plate as well as at the center O (Fig. 3) are presented in Table 5 for the fully clamped case. It is seen that the normal stresses σ_{xx} and σ_{yy} are in excellent agreement. Twelfth order polynomial in each of x and y is used in generating the displacement fields of 169 displacement nodes. Number of nodes used in the I-DEAS model is 1559. The deflection (w_0) at the center of the fully clamped plate from the present study and the I-DEAS are -0.8442×10^{-3} (m) and -0.8443×10^{-3} (m) respectively for the square patch load. For the all sides simply supported case, the values of w_0, $(\sigma_{xx})_0$ and $(\sigma_{yy})_0$ are calculated at the center $(0.0, 0.0)$ and are given as:

$$\begin{aligned}
& w_0 = -3.132\times10^{-3}\ (\text{m}), \quad (\sigma_{xx})_0 = (\sigma_{yy})_0 = -171.5\ (\text{Pa}) \quad (\text{present}),\\
& w_0 = -3.132\times10^{-3}\ (\text{m}), \quad (\sigma_{xx})_0 = (\sigma_{yy})_0 = -171.3\ (\text{Pa}) \quad (\text{I-DEAS}).
\end{aligned}$$

The deflection w_0 from the two sources for the circular patch load are -0.6615×10^{-3} (m) and -0.6613×10^{-3} (m) respectively. For the all sides simply supported case, the values of w_0, $(\sigma_{xx})_0$ and $(\sigma_{yy})_0$ are calculated at the center $(0.0, 0.0)$ and are given as:

$$\begin{aligned}
& w_0 = -2.483\times10^{-3}\ (\text{m}), \quad (\sigma_{xx})_0 = (\sigma_{yy})_0 = -134.0\ (\text{Pa}) \quad (\text{present}),\\
& w_0 = -2.483\times10^{-3}\ (\text{m}), \quad (\sigma_{xx})_0 = (\sigma_{yy})_0 = -134.2\ (\text{Pa}) \quad (\text{I-DEAS}).
\end{aligned}$$

Table 5
Stresses (Pa) in a partially loaded (square/circular patch $(x_0, y_0) = (0.25\ \text{m}, 0.25\ \text{m})$ square plate with built in edges

Location (x, y)	I-DEAS σ_{xx}	Present σ_{xx}	I-DEAS σ_{yy}	Present σ_{yy}
Square patch				
0.50,0.0	313.00	312.63	93.50	93.79
−0.50,0.0	72.87	72.35	22.18	21.71
0.0,0.50	93.50	93.79	313.00	312.63
0.0,−0.50	22.18	21.71	72.87	72.35
0.0,0.0	−59.50	−59.64	−59.50	−59.64
Circular patch				
0.50,0.0	246.50	245.91	73.63	73.77
−0.50,0.0	56.45	55.48	17.18	16.64
0.0,0.50	73.63	73.78	246.50	245.92
0.0,−0.50	17.18	16.64	56.45	55.48
0.0,0.0	−45.20	−44.98	−45.20	−44.98

$a = b = 1.0$ (m), $c = d = 0.25$ (m), $E = 1.0$ (MPa), $q = 1.0$ (Pa), $v = 0.3$ and $h = 0.01$ (m).

The agreement between the results from the present method and those from I-DEAS is very good for the above cases with patch loadings on the square plate and with opening in the square plate.

Circular and elliptic plates. In this section, a modeling procedure for the analysis of elliptic plates with the same load types and openings as the square plates is presented. The circular plate is a special case of the elliptic one. Fig. 4 shows appropriate geometric parameters for the plate as well as the circular and square patches which can be treated either as the loading areas or the openings. An elliptic plate is first mapped into a circle of radius unity using the transformation $x = a\cos\theta$ and $y = b\sin\theta$. Here, $a =$ the major axis, $b =$ the minor axis and $\theta =$ the angle from the positive x-axis. On and inside this circle, the geometric nodes, the number of which depends on the order of polynomials in ξ and η, are prescribed first to find the shape functions given in Eq. (11), which is then used to define displacement nodes. Using the displacement nodes, the shape functions in x and y as given in Eq. (12) are generated and used in the numerical calculations.

To understand the effects of the number of geometric nodes on the accuracy of the results, clamped and simply supported elliptic plates subjected to uniformly distributed loads are analyzed using 9, 16 and 25 geometric nodes. Numerical values of deflection and bending stresses (for the circular plate)/bending moments (for the elliptic plate) at points O, A and B as shown in Fig. 4 are presented in Tables 6 and 7

Table 6
Deflection (m) and Stresses (Pa) in a circular plate subjected to UDL on the lower face of plate

Parameter	Present method—geometric points			Exact solution
	9	16	25	
Clamped boundary conditions (*8th order polynomial*)				
w_0	−0.010228	−0.0107308	−0.0106855	−0.0106641
$(\sigma_{xx})_A$	−1659.51	−1875.58	−1874.00	−1875.00
$(\sigma_{yy})_A$	−507.99	−555.80	−561.52	−562.50
$(\sigma_{xx})_B$	−508.08	−555.90	−561.61	−562.50
$(\sigma_{yy})_B$	−1659.78	−1875.91	−1874.32	−1875.00
$(\sigma_{xx})_0$	1198.03	1211.21	1218.66	1218.75
$(\sigma_{yy})_0$	1198.03	1211.21	1218.66	1218.75
Simply supported boundary conditions (*10th order polynomial*)				
w_0	−0.041996	−0.0435972	−0.0435013	−0.0434766
$(\sigma_{xx})_0$	3025.93	3097.72	3093.99	3093.75
$(\sigma_{yy})_0$	3025.93	3097.72	3093.99	3093.75

Table 7
Bending moments in an elliptical plate with built in edges subjected to UDL

Parameter	Present method number of geometric nodes			Exact solution
	9	16	25	
Clamped boundary conditions				
w_0	−0.0036489	−0.0037899	−0.0037759	−0.0037592
$(M_x)_0$	−0.0091525	−0.0091256	−0.0092380	−0.0092266
$(M_y)_0$	−0.0137715	−0.0140048	−0.0140638	−0.0140477
$(M_x)_a$	0.0091648	0.0105601	0.0110124	0.0110159
$(M_y)_b$	0.0236693	0.0228876	0.0250052	0.0247907
Simply supported boundary conditions				
w_0	−0.0150390	−0.0155819	−0.0155463	−0.0155493
$(M_x)_0$	−0.0237780	−0.0240762	−0.0241004	−0.0246617
$(M_y)_0$	−0.0342234	−0.0351622	−0.0350654	−0.0356595

$a = 0.50$ m, $b = 0.33333$ m (12th order polynomial).

respectively for the uniformly loaded circular and elliptic plates for which exact results are available in the monograph of Timoshenko and Woinowsky-Krieger (1959). An excellent agreement between the results from the two different sources is found for both clamped and simply supported conditions. The case with 25 geometric nodes yields better results and hence this is used in the following calculations.

Clamped circular and elliptic plates subjected to patch loadings are analyzed by the present method using 14th order polynomial in each of x and y for the displacement fields. This requires 225 displacement nodes each having three degrees of freedom and the order of the resulting stiffness matrix is 675. The coordinates (x_0, y_0) of the centroids of the patch are: (0.1768 m, 0.1768 m) for the circular plate and $(b/2, b/2)$ for the elliptic plate. Circular and elliptic plates are also analyzed by I-DEAS using 1585 and 1934 nodes in the models respectively and the results are presented in Tables 8 and 9. The displacement w_0 at $(0.0, 0.0)$ are as follows.

Circular plate:

$$\text{Square patch load}: \; w_0 = -1.311 \times 10^{-3} \text{ (m) (present)} \quad \text{and} \quad w_0 = -1.319 \times 10^{-3} \text{ (m) (I-DEAS)},$$

$$\text{Circular patch load}: \; w_0 = -1.037 \times 10^{-3} \text{ (m) (present)} \quad \text{and} \quad w_0 = -1.045 \times 10^{-3} \text{ (m) (I-DEAS)}.$$

Table 8
Circular plate with built in edges subjected to uniformly distributed load on a patch with: $c = d = 0.25$ (m), for the square patch and $R = 0.125$ (m) for the circular patch $(x_0 = y_0 = 0.1768$ m)

Location (x, y)	I-DEAS σ_{xx}	Present σ_{xx}	I-DEAS σ_{yy}	Present σ_{yy}
Square patch				
0.50,0.0	301.00	298.51	89.65	89.64
−0.50,0.0	87.42	86.27	26.09	25.92
0.0,0.50	89.65	89.60	301.00	298.36
0.0,−0.50	26.09	26.08	87.42	86.82
0.0,0.0	−132.10	−132.80	−132.10	132.90
Circular patch				
0.50,0.0	237.10	232.35	70.66	69.77
−0.50,0.0	68.39	69.63	20.42	20.92
0.0,0.50	70.65	69.38	237.10	231.05
0.0,−0.50	20.42	21.48	68.39	71.51
0.0,0.0	−100.80	−99.33	−100.80	−99.36

Table 9
Stresses in an elliptical plate with built in edges subjected to UDL on the patch $((x_0, y_0) = (b/2, b/2))$, $c = d = 0.150$ m, $R = 0.075$ m, $a/b = 1.5$

Location (x, y)	I-DEAS σ_{xx}	Present σ_{xx}	I-DEAS σ_{yy}	Present σ_{yy}
Square patch				
0.50,0.0	33.56	32.50	10.04	9.78
−0.50,0.0	3.62	5.24	1.13	1.58
0.0,0.50	32.57	33.12	110.10	110.36
0.0,−0.50	10.63	10.87	35.52	36.21
0.0,0.0	−17.25	−18.22	−31.55	−32.11
Circular patch				
0.50,0.0	26.09	25.27	7.82	7.60
−0.50,0.0	2.79	4.17	0.87	1.26
0.0,0.50	25.54	25.90	86.42	86.30
0.0,−0.50	8.29	8.38	27.68	27.92
0.0,0.0	−13.10	−13.67	−24.36	−24.88

Elliptic plate:

Square patch load : $w_0 = -1.819 \times 10^{-4}$ (m) (present) and $w_0 = -1.815 \times 10^{-4}$ (m) (I-DEAS),

Circular patch load : $(w_0 = -1.424 \times 10^{-4}$ (m) (present) and $w_0 = -1.422 \times 10^{-4}$ (m) (I-DEAS).

Tables 10 and 11 present the values of stresses in the same manner as in Tables 8 and 9 respectively for the uniformly loaded circular and elliptic plates clamped at the boundary with square and circular openings. The values of displacement w_0 at $(0.0, 0.0)$ are:

Circular plate case:

Square hole : $w_0 = -10.47 \times 10^{-3}$ (m) (present) and $w_0 = -10.61 \times 10^{-3}$ (m) (I-DEAS),

Circular hole : $w_0 = -10.51 \times 10^{-3}$ (m) (present) and $w_0 = -10.59 \times 10^{-3}$ (m) (I-DEAS).

Elliptic plate case:

Square hole : $w_0 = -10.4722 \times 10^{-3}$ (m) (present) and $w_0 = -10.61 \times 10^{-3}$ (m) (I-DEAS),

Circular hole : $w_0 = -10.5128 \times 10^{-3}$ (m) (present) and $w_0 = -10.59 \times 10^{-3}$ (m) (I-DEAS).

Table 10
Circular plate with built in edges subjected to UDL

Location (x, y)	I-DEAS σ_{xx}	Present σ_{xx}	I-DEAS σ_{yy}	Present σ_{yy}
Square hole				
0.50,0.0	1821.00	1785.48	541.50	535.10
−0.50,0.0	1858.00	1879.99	549.20	563.45
0.0,0.50	541.60	535.73	1821.00	1787.58
0.0,−0.50	549.20	564.18	1858.00	1882.42
0.0,0.0	−1192.00	−1201.72	−1192.00	−1201.72
Circular hole				
0.50,0.0	1830.00	1802.91	542.90	540.33
−0.50,0.0	1861.00	1882.80	550.00	564.29
0.0,0.50	542.90	540.85	1830.00	1804.65
0.0,−0.50	550.00	564.79	1861.00	1884.46
0.0,0.0	−1196.00	−1206.83	1196.00	−1206.81

$c = d = 0.125$ m, $R = 0.0625$ m ($x_0 = y_0 = 0.1768$ m).

Table 11
Stresses in an elliptical plate with a hole ($(x_0, y_0) = (b/2, b/2)$), $c = d = 0.10$ m, $R = 0.05$ m, with built in edges subjected to UDL, $a/b = 1.5$

Location (x, y)	I-DEAS σ_{xx}	Present σ_{xx}	I-DEAS σ_{yy}	Present σ_{yy}
Square hole				
0.50,0.0	647.40	637.23	188.50	191.56
−0.50,0.0	659.30	649.53	190.40	195.25
0.0,0.50	434.90	446.24	1453.00	1486.98
0.0,−0.50	441.20	451.10	1477.00	1503.20
0.0,0.0	−553.30	−553.70	−843.60	−836.41
Circular hole				
0.50,0.0	645.60	640.74	186.30	192.61
−0.50,0.0	657.00	652.03	188.40	196.00
0.0,0.50	434.80	447.72	1455.00	1491.90
0.0,−0.50	439.20	451.88	1472.00	1505.77
0.0,0.0	−556.80	−553.67	−848.20	−837.60

Table 12
Stresses at the geometric center of a circular plate with a hole or patch ($x_0 = y_0 = 0.1768$ m) with simply supported edges subjected to UDL

Parameter	Present	I-DEAS	Present	I-DEAS
	Square patch		Circular patch	
w_0	−5.021e−03	−5.018e−03	−3.994e−3	−3.993e−03
$(\sigma_{xx})_0$	−346.80	−343.00	−269.91	−268.90
$(\sigma_{yy})_0$	−346.76	−343.00	−269.92	−268.90
	Square hole		Circular hole	
w_0	−0.04393	−0.04545	−0.04375	−0.04484
$(\sigma_{xx})_0$	−3102.51	−3083.00	−3103.53	−3076.00
$(\sigma_{yy})_0$	−3102.51	−3083.00	−3103.53	−3076.00

$c = d = 0.125$ m and $R = 0.0625$ m for the hole. $c = d = 0.25$ m and $R = 0.125$ m for the patch loading.

Table 13
Stresses at $(0.0, 0.0)$ in an elliptical plate with a hole ($(x_0, y_0) = (b/2, b/2)$) with simply supported edges subjected to UDL, $a/b = 1.5$. $c = d = 0.10$ m and $R = 0.05$ m for the hole

Parameter	Present	I-DEAS	Present	I-DEAS
	Square patch		Circular patch	
w_0	−8.074e−04	−8.107e−04	−6.414e−04	−6.415e−04
$(\sigma_{xx})_0$	−67.80	−67.06	−52.96	−52.62
$(\sigma_{yy})_0$	−100.33	−100.00	−78.57	−78.67
	Square hole		Circular hole	
w_0	−0.0157732	−0.0158900	−0.0157210	−0.0101574
$(\sigma_{xx})_0$	−1459.88	−1449.00	−1459.44	−1451.00
$(\sigma_{yy})_0$	−2127.93	−2132.00	−1459.44	−1451.00

$c = d = 0.15$ m and $R = 0.075$ m for the patch loading.

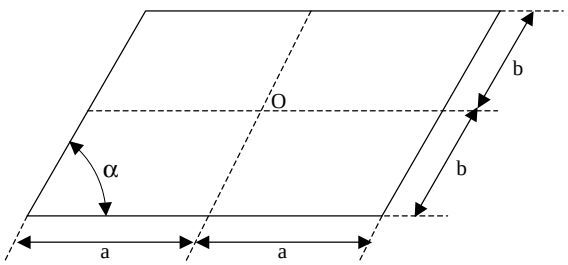

Fig. 6. Geometry of the skew plate.

Simply supported boundary condition with patch loadings and also other cases with square and circular openings are analyzed and results presented in Tables 12 and 13 respectively for the circular and elliptic plates. Results at the geometric center O are reported only, as the values of the stresses and displacement at points A through D are found to be negligibly small.

The values of the normal stresses σ_{xx} and σ_{yy} at points A–D and geometric center O of the plate as shown in Fig. 4 from the present method and also from I-DEAS are in very good agreement. In the case of the

Table 14
Simply supported rhombic plate subjected to uniform transverse load

	Morley (finite difference method)				Present			
α	n_i	w_0	M_{max}	M_{min}	$p(n_i)$	w_0	M_{max}	M_{min}
Simply supported case								
90	49	0.0443	0.0473	0.0473	(9)4	0.0448	0.0500	0.0500
	81	0.0443	0.0475	0.0475	(16)5	0.0448	0.0500	0.0500
	121	0.0443	0.0476	0.0476	(25)6	0.0444	0.0479	0.0479
	169	0.0443	0.0477	0.0477	(36)7	0.0444	0.0479	0.0479
					(49)8	0.0444	0.0479	0.0479
					(64)9	0.0444	0.0479	0.0479
80	121	0.0422	0.0485	0.0444	(9)4	0.0424	0.0495	0.0475
					(16)5	0.0426	0.0506	0.0464
					(25)6	0.0423	0.0483	0.0446
					(36)7	0.0423	0.0485	0.0446
					(49)8	0.0423	0.0486	0.0447
					(64)9	0.0423	0.0485	0.0448
60	121	0.0276	0.0427	0.0323	(9)4	0.0261	0.0400	0.0285
	169	0.0277	0.0427	0.0325	(16)5	0.0273	0.0416	0.0303
					(25)6	0.0277	0.0431	0.0324
					(36)7	0.0279	0.0426	0.0342
					(49)8	0.0280	0.0430	0.0346
					(64)9	0.0280	0.0431	0.0343
50	121	0.0182	0.0364	0.0245	(9)4	0.0161	0.0321	0.0186
					(16)5	0.0177	0.0336	0.0216
					(25)6	0.0183	0.0367	0.0256
					(36)7	0.0185	0.0371	0.0273
					(49)8	0.0186	0.0361	0.0266
					(64)9	0.0185	0.0359	0.0257
40	121	0.0100	0.0283	0.0165	(9)4	0.0081	0.0231	0.0110
	169	0.0101	0.0283	0.0168	(16)5	0.0094	0.0250	0.0139
					(25)6	0.0099	0.0282	0.0177
					(36)7	0.0100	0.0288	0.0185
					(49)8	0.0101	0.0279	0.0177
					(64)9	0.0105	0.0288	0.0177
30	49	0.0038	0.0189	0.0086	(9)4	0.0030	0.0141	0.0056
	81	0.0039	0.0191	0.0091	(16)5	0.0037	0.0161	0.0074
	121	0.0041	0.0192	0.0094	(25)6	0.0039	0.0183	0.0096
	169	0.0041	0.0192	0.0096	(36)7	0.0040	0.0185	0.0098
	225	0.0042	0.0192	0.0098	(49)8	0.0041	0.0186	0.0097
					(64)9	0.0039	0.0170	0.0085

n_i = number of internal nodes, p = the order of the polynomial.

elliptic plate with patch loadings, the magnitudes of the stresses are considerably small at point C (−0.50, 0.0 in Table 9) and the difference in the results from the two methods is seen in the range of 30–50%. The displacement w_0 is generally in excellent agreement for all of the above cases.

Skew plates. The present method is also evaluated against the results published by Morley (1963), who published a short monograph providing the theory of elastic structure that is needed to solve skew plate problems. The author provided analytical and finite difference solutions using polar and oblique coordinate systems respectively for the uniformly loaded skew plates as shown in Fig. 6. Both the simply supported and clamped boundary conditions were considered. Table 14 contains deflection w_0 in (m) and principal

Table 15
Simply supported rhombic plate subjected to uniform transverse load

	Morley (simple series solution)				Present			
α	N	w_0	M_{max}	M_{min}	p	w_0	M_{max}	M_{min}
Simply supported case								
85	3	0.0438	0.0484	0.0464	4	0.0442	0.0501	0.0491
	6	0.0438	0.0486	0.0466	5	0.0443	0.0507	0.0488
					6	0.0439	0.0484	0.0467
					7	0.0439	0.0486	0.0466
					8	0.0439	0.0485	0.0466
					9	0.0439	0.0486	0.0466
80	3	0.0423	0.0484	0.0448	4	0.0424	0.0495	0.0475
	6	0.0423	0.0486	0.0448	5	0.0426	0.0506	0.0464
					6	0.0423	0.0483	0.0446
					7	0.0423	0.0485	0.0446
					8	0.0423	0.0486	0.0447
					9	0.0423	0.0485	0.0448
60	3	0.0280	0.0427	0.0330	4	0.0261	0.0400	0.0285
	6	0.0280	0.0425	0.0333	5	0.0273	0.0416	0.0303
					6	0.0277	0.0431	0.0324
					7	0.0279	0.0426	0.0342
					8	0.0280	0.0430	0.0346
					9	0.0280	0.0431	0.0343
50	3	0.0186	0.0365	0.0251	4	0.0161	0.0321	0.0186
	6	0.0188	0.0362	0.0258	5	0.0177	0.0336	0.0216
					6	0.0183	0.0367	0.0256
					7	0.0185	0.0371	0.0273
					8	0.0186	0.0361	0.0266
					9	0.0185	0.0359	0.0257
40	3	0.0103	0.0284	0.0172	4	0.0081	0.0231	0.0110
	6	0.0105	0.0281	0.0180	5	0.0094	0.0250	0.0139
					6	0.0099	0.0282	0.0177
					7	0.0100	0.0288	0.0185
					8	0.0101	0.0279	0.0177
					9	0.0105	0.0288	0.0177
30	3	0.0043	0.0191	0.0101	4	0.0030	0.0141	0.0056
	4	0.0044	0.0192	0.0105	5	0.0037	0.0161	0.0074
	5	0.0044	0.0192	0.0107	6	0.0039	0.0183	0.0096
	6	0.0044	0.0191	0.0108	7	0.0040	0.0185	0.0098
	7	0.0045	0.0191	0.0108	8	0.0041	0.0186	0.0097
	8	0.0045	0.0191	0.0108	9	0.0039	0.0170	0.0085

N = number of terms in the series, p = the order of the polynomial.

bending moments M_{max} and M_{min}, both in (N m/m), at the center O of the plate obtained by the finite difference method in oblique coordinate system for skew angles 90–30°. The results are given against the number of internal grid points considered in the finite difference solution. The results from the present method are also presented in this table against number of internal displacement nodes. In Table 15, the results presented by Morley (1963) are obtained analytically using series solution in polar coordinate system. In general the agreement between the results from the two studies is very good. For small skew angles, the discrepancy is slightly higher in the neighborhood of 12%. The present method agrees better with the finite difference method used by Morley than the analytical method for the simply supported case.

Table 16
Clamped skew plates

	Morley					Present				
α	N	$a/b = 1.0$	$a/b = 1.25$	$a/b = 1.5$	$a/b = 2.0$	p	$a/b = 1.0$	$a/b = 1.25$	$a/b = 1.5$	$a/b = 2.0$
w_0										
75	2	0.0128	0.0178	0.0212	0.023	4	0.0026	0.0048	0.0077	0.0146
	4	0.0123	0.0176	0.0211	0.0242	5	0.0107	0.0164	0.0209	0.0262
	6	0.0122	0.0176	0.0211	0.0242	6	0.0120	0.0173	0.0209	0.0240
	8	0.0122				7	0.0122	0.0176	0.0211	0.0240
						8	0.0123	0.0176	0.0212	0.0242
						9	0.0123	0.0176	0.0212	0.0242
60	4		0.0122	0.0142	0.0158	4		0.0012	0.0018	0.0039
						5		0.0083	0.0107	0.0147
						6		0.0114	0.0137	0.0158
						7		0.0119	0.0141	0.0158
						8		0.0120	0.0142	0.0158
						9		0.0120	0.0142	0.0158
45	4			0.0068	0.0071	4			0.0006	0.0012
						5			0.0045	0.0060
						6			0.0064	0.0073
						7			0.0067	0.0073
						8			0.0067	0.0072
						9			0.0067	0.0071

N = number of terms in the series, p = the order of the polynomial.

However, the finite difference grid is much finer than the displacement grid used in the present analysis. The results for the uniformly loaded clamped plate are presented in Table 16 and the agreement is excellent. Here, Morley used the oblique coordinates in solving this problem.

4. Concluding remarks

A numerical method using the concept of the finite element method has been presented in this paper for the bending of complicated shaped plates. In this method the plate geometry and the displacements are expressed in terms of higher order polynomials. The method utilizes two sets of nodal points, the first needed for the coordinate interpolation and the second for defining the degrees of freedom. The method is truly numerical where the integration is carried out using as many Gauss points as needed according to the order of the polynomial used. It is unified in the sense that different complicated shaped plates can be analyzed using the same algorithm. Numerical examples of rectangular, circular, elliptical and skew plates with clamped and simply supported boundary conditions and subjected to uniformly distributed loads are considered in this study. Extremely favorable comparisons of the numerical results are made with the exact solution found in the monograph of Timoshenko and Woinowsky-Krieger (1959) and finite difference and simple series solutions presented by Morley (1963). Uniformly loaded square and elliptic plates with offset patch loadings, or with square and circular openings, are also analyzed and the results are compared with those from the finite element analysis. Both displacements and stresses are accurately predicted by the present method.

References

Bardell, N.S., 1996. An engineering application of the *h–p* version of the finite element method to the static analysis of a Euler–Bernoulli beam. Computers and Structures 59, 195–211.

Belytschko, T., Krongauz, Y., Organ, D., Fleming, M., Krysl, P., 1996. Meshless method: An overview and recent developments. Computer Methods in Applied Mechanics and Engineering 139, 3–47.

Belytschko, T., Lu, Y.Y., Gu, L., 1994. Element free Galerkin methods. International Journal of Numerical Methods in Engineering 37, 229–256.

Chen, X.L., Liu, G.R., Lim, S.P., 2003. An element free Galerkin method for the free vibration analysis of composite laminates of complicated shape. Computers and Structures 59, 279–289.

El Ouatouati, A., Johnson, D.A., 1999. A new approach for numerical modal analysis using the element-free method. International Journal for Numerical Methods in Engineering 46, 1–27.

Harik, I.E., Salamoun, G.L., 1986. Analytical strip solution to rectangular plates. Journal of Engineering Mechanics 112, 105–118.

I-DEAS Master Series™, Structural Dynamics Research Corporation, Milford, OH 45150.

Liew, K.M., Han, J.B., 1997. Bending analysis of simply supported shear deformable skew plates. Journal of Engineering Mechanics 123, 214–221.

Mohr, G.A., 2000. Polynomial solutions for thin plates. International Journal of Mechanical Sciences 42, 1197–1204.

Morley, L.S.D., 1963. Skew Plates and Structures. The Macmillan Company, New York.

Ollerton, E., 1976. Bending stresses in thin circular plates with single eccentric circular holes. Journal of Strain Analysis 11, 202–224.

Suetake, Y., 2002. Element free method based on Lagrange polynomial. ASCE Journal of Engineering Mechanics 128, 231–239.

Timoshenko, S., Woinowsky-Krieger, S., 1959. Theory of Plates and Shells. McGraw Hill Book Co, NY.

Venkatesh, A., Jirousek, J., 1995. Accurate representation of local effects due to concentrated and discontinuous loads in hybrid-Trefftz plate bending elements. Computers and Structures 57, 863–870.

Weaver, W., Johnston, P.R., 1984. Finite Elements for Structural Analysis. Prentice Hall, Englewood Cliffs, NJ.